

Discontinuous presentation of ambiguous figures: How interstimulus-interval durations affect reversal dynamics and ERPs

JÜRGEN KORNMIEIER,^{a,b} WERNER EHM,^b HEIKO BIGALKE,^a AND MICHAEL BACH^a

^aSektion Funktionelle Sehforschung, Universität-Augenklinik Freiburg, Freiburg, Germany

^bInstitut für Grenzgebiete der Psychologie, Freiburg, Germany

Abstract

If we observe an ambiguous figure, our percept is unstable and alternates between the possible interpretations. Periodically interrupting the presentation sizably modulates the spontaneous reversal rate. We here studied event-related potential (ERP) correlates of the neural processes underlying these strong modulations. An ambiguous Necker stimulus was presented discontinuously with four randomly varying interstimulus intervals (ISI; 14, 43, 130, 390 ms) while participants indicated perceptual reversals. EEG was selectively averaged with respect to the participants' percept and ISI. ERP traces varied markedly between ISIs. A simple model explained a major part of this variation and showed that the ISI-dependent ERP modulation occurs after disambiguation has already taken place. We suggest that perceptual stability (or reversal) depends on a system state, slowly changing from one reversal to the next. ISI can shift this state on a scale between stability and instability.

Descriptors: Ambiguous figures, Multistable perception, Bistable perception, Necker cube, Event-related potentials (ERPs), EEG

To produce a stable and unambiguous percept the available visual information needs to be disambiguated and interpreted. Ambiguous figures (e.g., the famous Necker cube; Necker, 1832) demonstrate impressively both the capability and the limitations of such perceptual processes: A physically unchanged visual object leads to sudden and spontaneous perceptual reversals. Understanding the mechanisms underlying this phenomenon promises insight into the mechanisms of object perception and object representation in general (Blake & Logothetis, 2002; Crick & Koch, 1998; Engel, Fries, & Singer, 2001; James, 1950).

A large number of results from psychophysical experiments with ambiguous figures evolved into two explanatory approaches, either assuming low-level visual adaptation (bottom-up approach) or cognitive/attentional mechanisms near awareness (top-down approach) as the causal factors (for a review, see Long & Toppino, 2004). In the last two decades several physiological and fMRI studies with ambiguous figures have been performed. Imaging studies report reversals to be accompanied by activation of specific brain areas and deactivation of others (Inui et al., 2000; Kleinschmidt, Buchel, Zeki, & Frackowiak, 1998; Müller et al., 2005). However it is still unclear which of the underlying neural processes initiate a perceptual reversal and which are secondary.

The temporal order of neural processes underlying a perceptual reversal may be assessed with the EEG (and especially with event-related potentials, ERPs) thereby benefiting from their high temporal resolution. For averaging ERPs, however, the precise time point of the perceptual reversal is necessary but difficult to access in the case of an endogenous event such as a spontaneous perceptual reversal. Two different experimental paradigms were invented to overcome this problem, namely backward averaging from subjects' manual responses (e.g., Basar-Eroglu, Strüber, Stadler, & Kruse, 1993; Strüber & Herrmann, 2002) and forward averaging from stimulus onset using discontinuous stimulus presentation (Kornmeier & Bach, 2004, 2005, 2006; Kornmeier, Heinrich, Atmanspacher, & Bach, 2001; O'Donnell, Hendler, & Squires, 1988; Pitts, Nerger, & Davis, 2007). While early occipital ERP correlates of perceptual reversals provided support for the bottom-up approach (e.g., Kornmeier & Bach, 2004, 2005), P300-like components seemed to indicate cognitive (top-down) processes underlying perceptual reversals (e.g., Basar-Eroglu et al., 1993; O'Donnell et al., 1988). Kornmeier and Bach (2006) recently reported on a chain of event-related potentials related to perceptual reversals. They presented an ambiguous Necker stimulus discontinuously and compared ERP data related to endogenous perceptual reversals with data to exogenous reversals induced by physically alternating two unambiguous stimulus variants with opposite orientations. The two types of reversals were accompanied by two chains of ERP components that differed in two aspects: (1) An early occipital component (130 ms after stimulus onset) was restricted to the endogenous reversal,

Support by the Deutsche Forschungsgemeinschaft (BA 977-11) is gratefully acknowledged.

Address reprint requests to: Jürgen Kornmeier, Sektion Funktionelle Sehforschung, Universität-Augenklinik Freiburg, Killianstraße 5, 79106 Freiburg, Germany. E-mail: juergen.kornmeier@uni-freiburg.de

whereas (2) all subsequent components (including a P300-like parietal component) occurred also with exogenously induced reversals, however with reduced latency (40 ms to 100 ms) compared to their endogenous counterparts. The authors interpreted their results as follows: The early occipital positivity reflects the initial instability of the perceptual system caused by the ambiguous stimulus. The latency increase of the subsequent posterior negativity of about 40 ms in the case of the ambiguous compared to the unambiguous stimuli may estimate the time necessary for disambiguation (“disambiguation time”; Kornmeier & Bach, 2005). This second ERP component was assumed to reflect Gestalt reconstruction of the rivaling, or reversed, percept. Kornmeier and Bach integrated the different experimental results using reaction times as a common time reference for the ERP data from different averaging methods across ERP studies. They identified their parietal and frontopolar positivities as the P300-like component common to all ERP studies and attributed the absence of the earlier components in the backward-averaging studies to the high temporal jitter introduced by reaction times. According to their findings and in agreement with Strüber and Herrmann (2002), they interpreted the P300 as an index of awareness of the reversed percept rather than a direct correlate of the neural processes underlying the reversal.

Recently one particularly impressive bottom-up feature of multistability, which was initially demonstrated by Orbach, Ehrlich, and Heath (1963), has regained scientific interest (Brodeur, Lepore, Veilleux, Alyanak, & Debruille, 2006; Grossmann & Dobbins, 2006; Kornmeier, Heinrich, & Bach, 2002; Leopold, Wilke, Maier, & Logothetis, 2002; Maier, Wilke, Logothetis, & Leopold, 2003): Presenting the ambiguous stimulus discontinuously can strongly modulate the rate of perceptual reversals (“reversal rate”), mainly as a function of the ISI. Increasing the ISI from 0 (continuous observation) to about 400 ms raises reversal rates monotonously to more than twice the rate than during continuous observation (Figure 1, Kornmeier et al., 2002; Orbach et al., 1963; Orbach, Zucker, & Olson, 1966). At longer ISIs, the reversal rates decrease down to near zero (Leopold et al., 2002; Maier et al., 2003). These strong effects have been confirmed by several psychophysical studies, but no physiological correlates have been reported so far to our knowledge.

In the present study we thus searched for ERP correlates of the neural mechanisms underlying the strong increase of reversal rates with increasing ISIs. We recorded the EEG while presenting

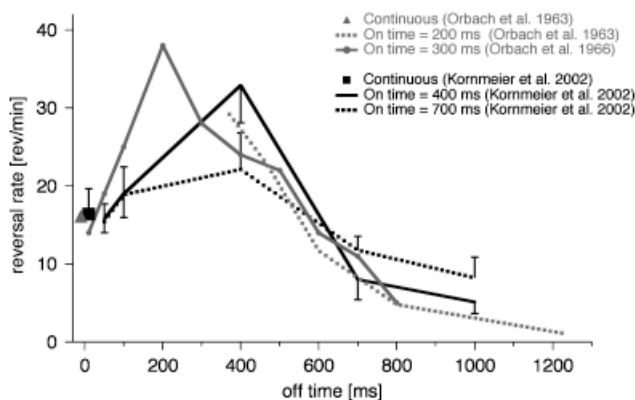


Figure 1. Reversal rates during continuous and discontinuous presentation of ambiguous Necker stimuli. Overview of results from three experimental studies.

the Necker lattice discontinuously with four randomly varying ISIs and compared associated chains of ERP components. Discrepancies between ERP traces may shed some light on the neural mechanisms underlying the increase of reversal rate. Further, the latencies when the ERP traces differ in dependence of the ISI may help to understand the functional role of the neural processes underlying the single steps of the ERP chain related to perceptual reversal. We found that ERP traces vary substantially between the four ISIs. However, a simple model explains a major part of that variation and indicates that the corresponding ERP chains are identical up to an amplitude modulation of the later components. This in turn suggests that two separate types of processes are at work: (1) slow (about 4 s) processes of destabilization leading to perceptual instability and (2) fast processes of disambiguation (around 40 ms) leading to a stable reversed percept. Because ISIs do not affect the latter, they may exert their impact on the former.

Methods

Participants

Twelve participants aged from 20 to 26 with a mean age of 23.5 years took part in the experiment. They were all naïve as to the specific experimental question and gave their informed written consent. All of them had normal or corrected-to-normal visual acuity. The study was performed in accordance with the ethical standards laid down in the Declaration of Helsinki (World Medical Association, 2000) and was approved by the local ethics review board.

Stimuli

The ambiguous stimulus was a “Necker lattice,” consisting of 3×3 Necker cubes. The stimulus was presented with a frame rate of 70 Hz at a viewing angle of $7.5^\circ \times 7.5^\circ$. Luminance of the lattice was 20 cd/m^2 ; background luminance was 0.01 cd/m^2 .

Procedure

The Necker lattice was presented discontinuously with 800 ms presentation time plus or minus an additional time interval varying with integer steps randomly between 14 and 100 ms to prevent potential habituation effects. Each presentation of the Necker lattice was followed by one of four randomly chosen ISIs (14, 43, 130, 390 ms), all of which appeared equally often. Participants compared the perceived front–back orientation of each Necker lattice with the previous one (“observation sequence”) and indicated by a key press with different hands the two different directions of perceived reversal. In separate experimental blocks they indicated by pressing with the left and right hand different keys perceived stability of each of the two possible orientations (Figure 2). After each key press the following ISI was prolonged to 1000 ms and the observation sequence restarted. Thus participants never compared a stimulus directly before a manual response with one directly after that response. Participants were instructed to gaze at a fixation cross in the center of the screen, not to provoke reversals volitionally, and to respond only if they were certain about their percept. The instructions included the statement that reversal and stability were equally important. With each participant the experiment was performed twice on two separate days.

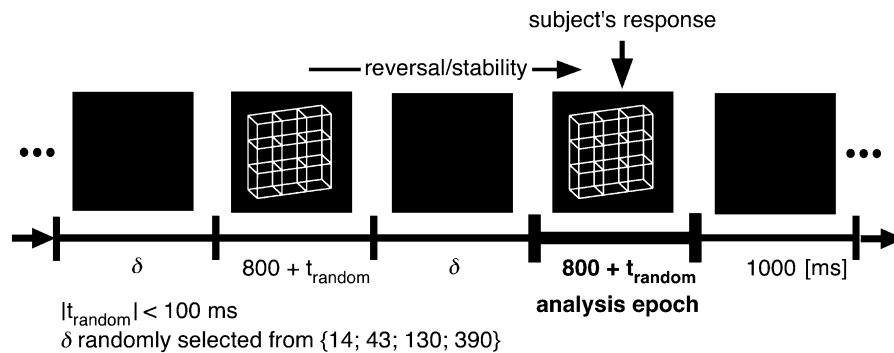


Figure 2. Experimental paradigm. Necker stimuli were presented for approximately 800 ms followed by a blank-screen ISI randomly chosen out of four possible values. Participants compared the front–back orientation of each stimulus with the preceding one (“observation sequence”) and indicated in separate blocks either perceived reversals or unchanged percepts by a key press. After each key press the ISI was prolonged to 1000 ms and a new observation sequence started.

EEG Recording

EEG was recorded from 13 gold-cup scalp electrodes at O1, O2, Oz, P3, P4, Pz, T3, T4, Cz, Fz, Fp3, Fp4, Fpz (American Encephalographic Society, 1994), referenced to the mean potential of both ears. Vertical and horizontal EOG electrodes detected eye movements and blinks. Signals were amplified and filtered (first-order band-pass 0.3–70 Hz) and digitized with a resolution of 12 bits at a sampling rate of 500 Hz. They were streamed to disk and also averaged online.

Data Analysis: EEG Data

The sweeps were automatically rejected in the case of artifacts from eye movements and amplitude excursions exceeding 100 μ V. They were averaged per condition and digitally filtered with a latency-neutral low-pass at 20 Hz. Peak amplitude was measured relative to baseline, which was defined as the average from 70 ms before to 30 ms after stimulus onset.

Eight different kinds of EEG epochs after stimulus onset were averaged separately. They were characterized by the type of percept that participants had reported (“perception type”: stability or reversal) and by the ISI preceding the participants’ response. EEG epochs from different presentation times and different response sites (right hand or left hand) were pooled together.

For each channel and ISI we computed a difference trace (reversal minus stability), which will be denoted as “dERP” below. ERP components related to low-level processing should thus be cancelled out. This resulted in a total of 52 (= 13 electrodes \times 4 ISIs) difference traces. Because not all components were unequivocally identifiable in every participant, we proceeded (as in previous studies) as follows: The four significant peaks reported in Kornmeier and Bach (2006) served as the center of a time window of 100 ms for early components with latencies shorter than 200 ms, and of 200 ms for later components. Then for each participant, the largest excursion in this time window defined the individual peak. The amplitudes and latencies of the dERP components were analyzed by repeated measurement MANOVAs with the factors ISI (ms: 14, 43, 130, 390) and Channel (averaged occipital, averaged parietal, averaged temporal, central, frontal, averaged frontopolar position) and the variables latency and amplitude. For the two late positive dERP components (parietal and frontopolar positivity) the time windows overlap. We therefore used a common time window for both and tested for latency differences between parietal and frontopolar electrode positions. In all cases of more than one

degree of freedom, we corrected according to Geisser and Greenhouse (1958). The original degrees of freedom and the corrected probability level are reported together with effect sizes (partial eta squared: η_p^2).

Data Analysis: Reversal Rates

In most studies on ambiguous figures, reversal rates are reported as the number of reversals relative to observation time (“reversals per minute,” e.g., Orbach et al., 1963). In the present study we aimed to compare reversal rates across the four different ISIs. Because ISIs changed randomly over time, it is not appropriate to report the number of reversals relative to observation time. Instead we counted for each ISI the number of reversals following that ISI and related these numbers of reversals to the total number of occurrences of the corresponding ISI. Then the null hypothesis of independence of reversal rate and ISI was tested by a randomization test (Achim, 1995; Edgington, 1995). Randomization tests generate their reference distribution by permuting the pooled original data. They require less assumptions than an ANOVA.

Data Analysis: Reaction Times

Reaction times were calculated as the time period between stimulus onset and the participants’ key press. We tested the null hypothesis of independence of reaction times and ISI by a randomization test (Achim, 1995; Edgington, 1995).

Results

Reversal Rates

The reversal rates at different ISIs (number of reversals following a special ISI vs. the number of occurrences of the specific ISI) can be seen in Figure 3, top. Reversal rates significantly increased with increasing ISI (δ) as reported in previous studies (Kornmeier et al., 2002; Orbach et al., 1963, 1966). Results of pairwise comparisons (t tests, corrected for multiple testing according to Holm, 1979) are shown in Table 1.

Reaction Times

Reaction time results are given in Figure 3, bottom. We observed no significant effects of ISI on reaction times.

Electrophysiological Results

The ERP traces for selected electrode positions (Oz, Pz, and Fpz) are presented in Figure 4. Strong differences between electrode

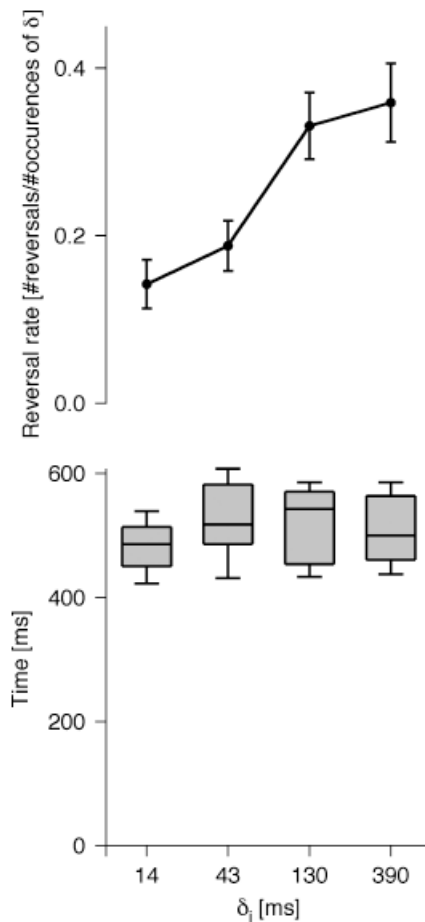


Figure 3. Psychophysical results. Top: Mean reversal rates (mean number of reversals following one ISI in relation to the number of occurrences of that specific ISI) increase significantly with increasing ISI. Abscissa with logarithmic scaling. Bottom: Median reaction times (horizontal lines) with 50th-percentile ranges (boxes) and 90th-percentile ranges (between whiskers). Reaction times of participants’ responses after perceived reversals do not differ significantly between ISIs (δ_i).

positions as well as between different ISIs can be observed. The occipital electrodes have in common that their stability traces deviate from the reversal traces at around 100 ms. Amplitudes at these electrodes are higher for the stability traces compared to the reversal traces in the time interval between 200 and 400 ms. All subsequent analyses operate on the differences of these traces (the dERPs).

The dERP traces for all ISIs and all electrode positions are presented in Figure 5A (Figure 5B will be addressed in the section “Modeling the ISI Effect” below). Colors indicate dERP traces pertaining to the particular ISIs. At first glance, a remarkable

Table 1. *p* values for reversal rates regarding the ISIs (* $p < 0.05$; ** $p < 0.01$).

δ	14	43	130	390
14				
43	*			
130	**	*		
390	**	**		

variability between the difference traces belonging to the different ISIs can be observed. A closer look reveals that the earliest significant component is a positivity at around 130 ms, most prominent at the occipital locations, $F(5,55) = 9.75$, $p < .001$, $\eta_p^2 = 0.47$, for the factor Channel, concerning the variable amplitude. This positivity is distinctive at the occipital and parietal electrode positions for all but the longest ISI (390 ms). In the latter case a remnant of that positivity persists as a shoulder in the left flank of the contiguous negativity at about 130 ms, $F(15,165) = 2.53$, $p = .054$, $\eta_p^2 = .187$, for the interaction ISI \times Channel concerning the variable amplitude. Following the early positivity, a broad negativity occurs at around 300 ms and is most prominent at posterior and central electrode positions, $F(5,55) = 9.34$, $p < .01$, $\eta_p^2 = .459$, for the factor Channel, concerning the variable amplitude. It occurs slightly earlier at the occipital positions than at the central position, $F(5,55) = 8.7$, $p < .001$, $\eta_p^2 = .442$, for the factor Channel, concerning the variable latency. Its latency is negatively correlated with ISI, $F(3,33) = 7.62$, $p < .01$, $\eta_p^2 = .409$, for the factor ISI, concerning the variable latency, which can be seen most clearly at the occipital left (O1) and right (O2) electrode positions. Further, at the posterior electrodes the amplitude of this negativity is progressively enlarged with increasing ISI, $F(15,165) = 7.26$, $p < .001$, $\eta_p^2 = .398$, for the interaction ISI \times Channel, concerning the variable amplitude.

The negativity is followed by positive excursions, most prominent for the two longer ISIs, $F(3,33) = 7.58$, $p < .01$, $\eta_p^2 = .408$, for the factor ISI concerning the variable amplitude and at parietal, central, and frontopolar positions, $F(15,165) = 3.31$, $p < .05$, $\eta_p^2 = .231$, for the interaction Channel \times ISI concerning the variable amplitude. The latency of the frontopolar positivity appears to be smaller compared to the latency of the parietal positivity; this latency difference is, however, not significant.

Discussion

Presenting a Necker stimulus discontinuously with randomly varying ISIs leads to strong modulations of the reversal rates, confirming results from earlier studies (Kornmeier et al., 2002; Orbach et al., 1963). The dERP traces exhibited four successive dERP components pertaining to perceptual reversals. All of them were modulated by varying ISIs: The amplitude of an early occipital positivity was strongly reduced in the case of the longest ISI compared to the three shorter ISIs, where it stayed unchanged. With increasing ISIs, the amplitude of the subsequent negativity was increased while its latency was reduced. Further the amplitudes of the two subsequent positivities were modulated with increasing ISI while reaction times stayed unaffected.

Are the dERPs Confounded with the Response to Stimulus Offset at Short ISIs?

When presenting a visual stimulus discontinuously, stimulus offset elicits early visual ERP signatures, beginning at around 100 ms after offset (Regan, 1989). At the two shorter ISIs (14 and 43 ms) the potentials related to the offset of the preceding stimulus (offset potentials) overlap with the early visual onset potentials from the subsequent stimulus, which are expected to begin between 60 ms and 100 ms after stimulus onset. Are the dERP discrepancies between ISIs the result of such effects?

We assume some degree of linearity, namely, that the offset potentials are independent of ISI and are not affected by the

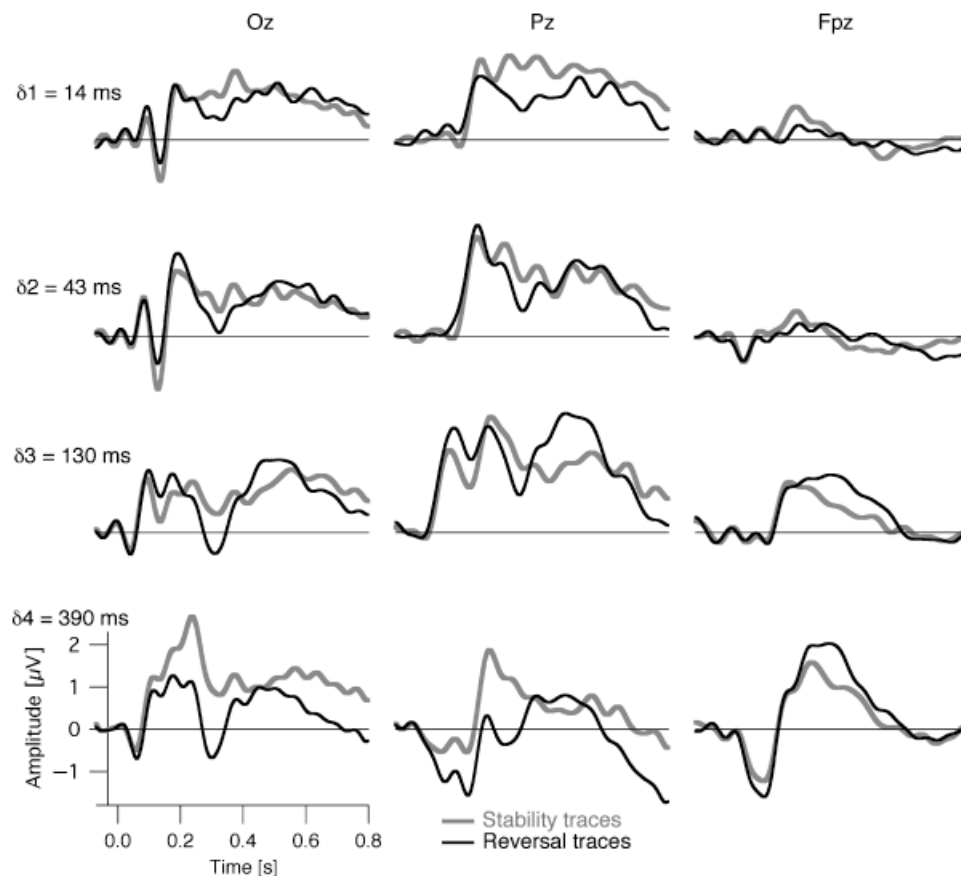


Figure 4. ERP traces (before subtraction). Each graph contains the ERP traces correlated with perceived reversals (black) or perceived stability (gray) of subsequent Necker lattices. Each column contains the graphs from one specific electrode position (indicated at the top). Each row contains the graphs for one of the four different ISIs (δ_i ; indicated on the left). The dERPs analyzed later are calculated as the difference (reversal minus stability) of these traces.

perceived orientation of the preceding stimulus. Offset potentials would then be additively superimposed on the overlapping stimulus-related potentials. Because our dERP signatures result from subtraction of two ERP traces (reversal condition minus stability condition), such effects would vanish to first order and only the correlates of perceptual reversals would remain. Any discrepancy between the dERP patterns at different ISIs will thus result from the impact of the ISIs onto neural processing underlying perceptual reversals and task execution.

Relation to Previous ERP Findings

The present data seem inconsistent in a few respects with results from earlier studies of ambiguous figures. Kornmeier and Bach (2004, 2005) had used an experimental paradigm that is very similar to the longest ISI condition of the present paradigm (ISI = 390 ms). Figure 6A compares the data from Kornmeier and Bach (2005) with the present data (Figure 6B represents further analyses of these data, as described in “Modeling the ISI Effect” below; it should be ignored for now). Both discrepancies and similarities between the two data sets can be observed:

1. An early occipital positivity can be seen in Kornmeier and Bach’s (2005) results (“Reversal Positivity” or “RP”). In the current results this deflection is present, but superimposed (in this longest ISI condition) by a slow negative component, starting at ≈ 50 ms (Figure 6A, bottom).

2. Subsequent to the early occipital positivity, an occipital/parietal negativity appears in Kornmeier and Bach’s (2005) results (“Reversal Negativity” or “RN”). A similar component is visible here, but extended to central and frontal electrode positions (Figure 6A, gray dERP traces) and it seems to occur slightly later in latency (280 ms vs. 260 ms).
3. The frontopolar positivity from Kornmeier and Bach’s (2005) study is very similar to the frontopolar positivity in the present data, whereas the present parietal positivity seems to be partly superimposed by a prominent slow negative component.

The discrepancies between the two data sets could be explained by two assumptions: (a) We suggest that some residual Bereitschaftspotential (“BP,” Kornhuber & Deecke, 1965) is superimposed on the reversal-related components in the present results: In the 2005 experiment the manual response was postponed until the subsequent ISI, thus sufficiently postponing the BP. Although the BP normally results from backward averaging with respect to movement onset, this slow wave may survive a potential time jitter of about 200 ms (interquartile range of the reaction times) if the EEG data are averaged forward from stimulus onset. In the present study, the timing is such that a BP would occur within the analysis epoch. It should, in principle, vanish when calculating the difference trace. However, because the BP is not solely related to preparation of motor activity but is also

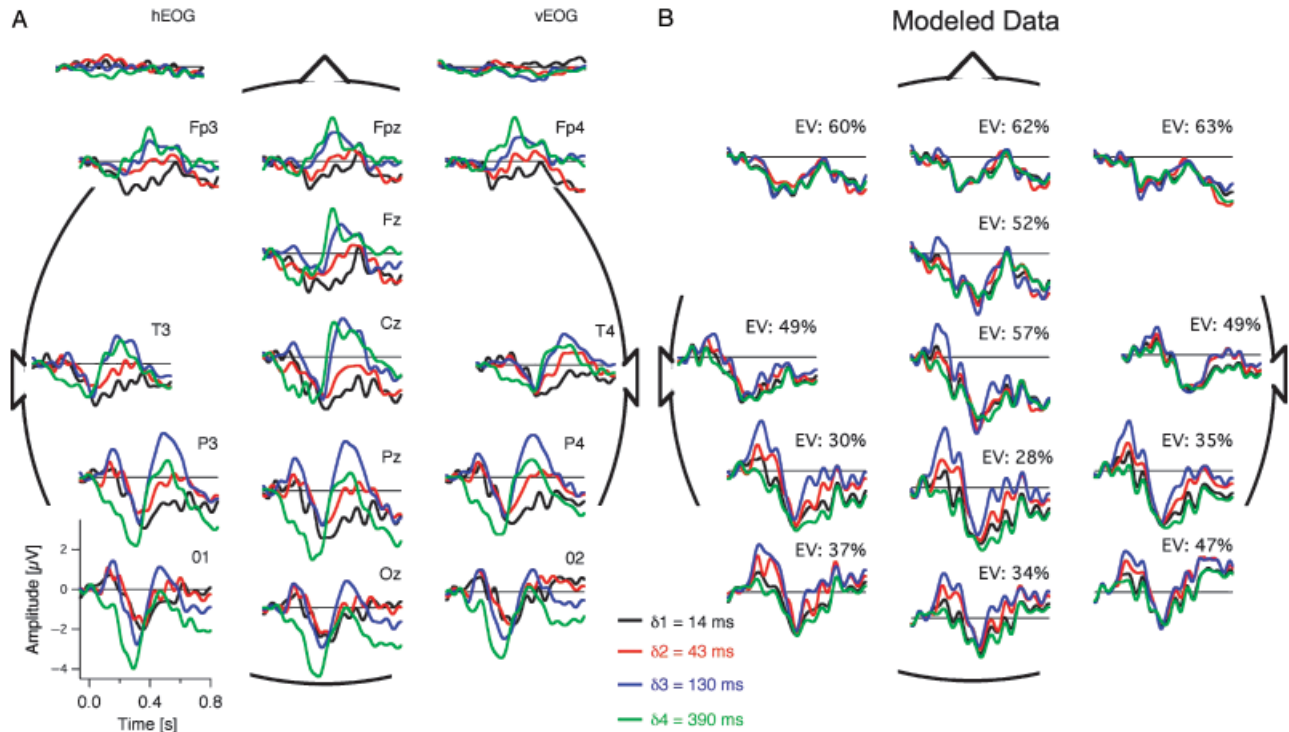


Figure 5. A: dERPs (ERP difference traces: reversal minus stability). Each color represents the grand mean dERP trace from 12 participants, corresponding to one specific ISI (δ_i). Varying ISIs introduce substantial variation between difference traces. B: Explained variance by application of a simple model (1) described in “Modeling the ISI Effect.” A simple model explains much of the variance observed in A. For each δ_i , the ISI-adjusted profile $A(\delta_i, t)$ represents a candidate for the ISI-independent profile $P_1(t)$. The degree of similarity of the four profiles $A(\delta_i, t)$ indicates how much of the variance from A can be explained by the model from Equation (1). EV: explained variance.

influenced by the level of attention or concentration (Birbaumer, Elbert, Canavan, & Rockstroh, 1990), it may differ between reversal and stability conditions due to different vigilance or attentional state. Consequently, a residual BP may be present and may explain the prominent negative excursions at the temporal, central, and frontal electrode positions. (b) Higher ISIs are correlated with an increase in amplitude and a decrease in latency of the Reversal Negativity (Figure 5A, O1 and O2 electrodes). Further, ISIs modulate the subsequent parietal positivity (Figure 5A, parietal electrodes). We assume that an increase of the Reversal Negativity’s amplitude is accompanied by broadening and thus by more overlap with the subsequent parietal positivity. The broader overlap may explain the observed latency modulation of the Reversal Negativity. It may further explain the lower amplitude of the parietal positivity for the longest ISI at the parietal electrode, where the Reversal Negativity is still prominent, compared to its amplitude at the central electrode, which is less affected by the Reversal Negativity (e.g., Kornmeier & Bach, 2004).

In the case of the longest ISI an overlap of the Reversal Negativity with the preceding Reversal Positivity may explain its shift toward negative amplitude values.

This explanation, however, assumes a more prominent Reversal Negativity in the present data compared to our 2005 study, where the Reversal Positivity is unaffected by the subsequent Reversal Negativity. Why should this be the case, since the paradigms are very similar? We cannot explain this sufficiently at the moment but speculate as follows: In the present study (response during stimulus presentation) participants had much

less time for perceptual analysis and response preparation than in the 2005 study (response in the ISI after stimulus offset). A shorter time for perception and task execution may lead to increased attention/concentration, potentially accompanied by higher neural activity due to higher arousal.

Modeling the ISI Effect

We modeled the dERPs by a (weighted) superposition of two profiles, P_1, P_2 , the first of which is independent of ISIs whereas the second is modulated by ISIs in such a manner that its amplitude is progressively amplified with increasing ISI (see the second-to-last paragraph in the “Results” section). Specifically we propose the following simple model for the dERPs $R(\delta_i, t)$ pertaining to ISI δ_i :

$$R(\delta, t) = P_1(t) + (1 - e^{-\alpha\delta_i}) \cdot P_2(t) + \varepsilon(t). \quad (1)$$

The profile $P_2(t)$ and the scaling parameter α can be estimated by the method of least squares (see the Appendix):

$$P_2(t) = \frac{\sum_{i,k} (R(\delta_i, t) - R(\delta_k, t)) \cdot (e^{-\alpha\delta_i} - e^{-\alpha\delta_k})}{\sum_{i,k} (e^{-\alpha\delta_i} - e^{-\alpha\delta_k})^2}.$$

For each δ_i the ISI-adjusted profile

$$A(\delta_i, t) = R(\delta_i, t) - (1 - e^{-\alpha\delta_i})P_2(t) \quad (2)$$

represents a candidate for the ISI-independent profile $P_1(t)$, and we estimate the latter by the average of the $A(\delta_i, t)$. Remaining differences between the $A(\delta_i, t)$ reflect effects not represented by

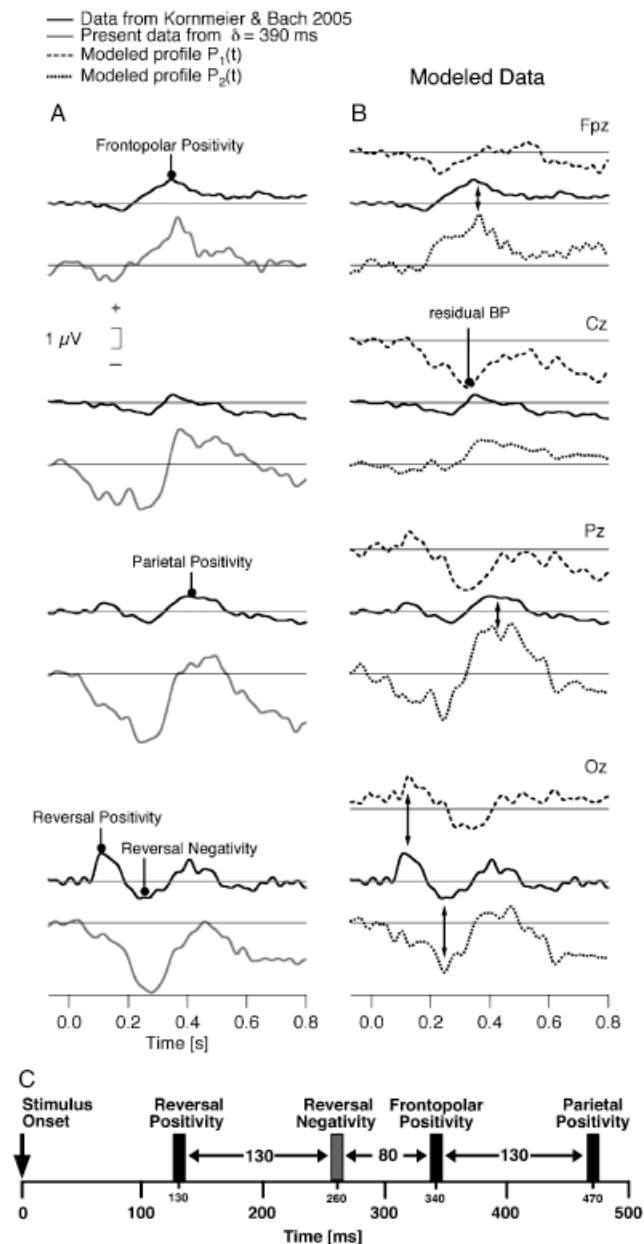


Figure 6. A: Comparison of the present results with former findings. The present paradigm and that from Kornmeier and Bach (2005) differ mainly in the time point of the participants' response. In the present data ($\delta = 390$ ms) a prominent negativity occurs at Cz and the Reversal Positivity is strongly reduced at Oz compared to Kornmeier and Bach's data. B: Comparison of the model results with former findings as analyzed in "Modeling the ISI Effect." After decomposition of the difference traces to the profiles $P_1(t)$ (independent of ISI) and $P_2(t)$ (dependent on ISI), the occipital $P_1(t)$ exhibits the Reversal Positivity and the central $P_1(t)$ a negativity reminiscent of the BP. $P_2(t)$ contains the residual components from the dERP chain (C, from Kornmeier & Bach, 2006, modified).

our model and residual noise. Figure 5B shows that the adjusted profiles are surprisingly similar and that our model explains a substantial amount of the variance.

Figure 6B shows the $P_1(t)$ and the weighted $P_2(t)$ (for $\delta = 390$ ms) in relation to results from Kornmeier and Bach (2005). $P_1(t)$ contains a negativity that is maximal at central and parietal electrode positions and that may represent a residual Bereit-

schaftspotential (BP). $P_1(t)$ further contains an early positivity at around 130 ms at occipital and parietal electrode positions with a maximum at the occipital pole (Figure 6B). The positivity is strongly reminiscent of the Reversal Positivity (RP), the earliest dERP component in Kornmeier and Bach's chain of dERP components (Kornmeier & Bach, 2006; see also Figure 6C). In fact, a cross-correlation analysis, using the RP from Kornmeier and Bach (2005) as template, reveals a maximal correlation coefficient $r_{\max} = 0.95$, $p < .001$, at a time lag $\Delta t = 18$ ms.

Likewise, the dERP components from $P_2(t)$ are very similar in sign, distribution, and latency to those found in the chain of reversal related dERP components (Kornmeier & Bach, 2006): A posterior negativity at around 250 ms, similar to Kornmeier and Bach's Reversal Negativity, $r_{\max} = 0.93$, $p < .001$, $\Delta t = 4$ ms, was followed by a frontopolar positivity at around 360 ms, $r_{\max} = 0.77$, $p < .001$, $\Delta t = 26$ ms, and a parietal positivity at around 460 ms, $r_{\max} = 0.88$, $p < .001$, $\Delta t = 4$ ms, similar to the late positivities in Kornmeier and Bach (2006) that occur in $P_2(t)$ (Figure 6B, C).

Thus the dERP components of Kornmeier and Bach's (2006) processing chain are not diluted by getting apportioned to both profiles in our model. Rather they are classified uniquely by appearing in either $P_1(t)$ or $P_2(t)$, hence as being either immune to ISI variation (RP, BP) or affected by ISI variation (RN and late positivities). What does this mean with regard to the underlying perceptual reversal process?

The present findings, unfortunately, throw little light on the ISI-dependent modulation of reversal rates if we accept assumptions from Kornmeier and Bach (2006) concerning the temporal order of the disambiguation process: According to the present model, ISI has no influence on dERP components in the time interval of the disambiguation process. Kornmeier and Bach (2005, 2006) suppose that disambiguation of the visual information takes about 40 ms and has finished before 250 ms after stimulus onset. The earliest ISI-dependent dERP modulation occurs at around 250 ms, and thus after disambiguation of the ambiguous visual information has already taken place.

The above considerations invite two alternative explanations of the present results: (1) Although ISIs do affect the reversal process in the critical time period before 250 ms after stimulus onset, this is not visible in the dERPs. (2) Multistable perception consists of two separate types of processes: (a) Processes underlying disambiguation of the visual information from an initial perceptual instability toward a reversed stable percept; these seem to be unaffected by ISIs. (b) Processes driving the perceptual system to such an initial instability, which seems to be the prerequisite of a perceptual reversal. These may be slow state changes, developing over several stimulus presentations and being sensitive to ISIs and adaptation. However, the extended time spans relevant for such state changes were not in the focus of the present study. Similar assumptions of slow state changes were proposed in the context of those explanatory approaches emphasizing the role of adaptation or satiation (e.g., Orbach et al., 1963) and by a recent MEG study from Strüber and Herrmann (2002). One can easily imagine that top-down influences like volitional control (e.g., Pelton & Solley, 1968; Toppino, 2003) accelerate or decelerate the changes in perceptual state.

How can we interpret the strong ISI-dependent modulations of the dERPs after 250 ms? According to the former assumptions, these occur after disambiguation and are thus likely to be related to task execution, like retrieval of iconic memory, which may be necessary to perform the comparison between the

previous and the actual percept of successively presented Necker stimuli. We speculate that in the case of a reversed percept, the retrieval process may be more “expensive,” leading to higher amplitudes of corresponding ERP components. Leopold et al. (2002) recently emphasized the role of memory in the context of multistable perception. Di Lollo, Enns, and Rensink (2000) demonstrated that ISIs between 100 ms and 300 ms are critical for iconic memory. In this context the negativity reminds us of the visually evoked mismatch negativity that is automatically evoked by stimuli that deviate from the previous stimuli (e.g., Alho, Woods, Algazi, & Näätänen, 1992) and is also discussed in the context of short term memory (Näätänen, 1990). However, whereas the amplitude of the visual mismatch negativity decreases with increasing ISI (Fu, Fan, & Chen, 2003), the present occipital/parietal negativity develops in the opposite direction. Further, there is evidence for memory-related ERP positivities in the time range of the present parietal and frontopolar positivity

(e.g., Boehm, Sommer, & Lueschow, 2005; Sommer, Heinz, Leuthold, Matt, & Schweinberger, 1995).

Conclusion

If an ambiguous Necker stimulus is presented discontinuously, the rate of perceptual reversals strongly varies with ISI. We here studied ERP correlates of the neural processes underlying this modulation. Strong effects on the dERPs were found, which could be decomposed into ISI-independent and ISI-dependent effects. The latter only occur after 250 ms, too late to explain the strong ISI-dependent modulation of reversal rates.

Possibly, perceptual stability decays due to slow state changes (maybe over several stimulus presentations) whose phase is susceptible to ISI. The role of slow state changes for multistable perception could be tested in experiments comparing top-down influences (e.g., attention) to bottom-up influences (e.g., ISI-related adaptation).

REFERENCES

- Achim, A. (1995). Signal detection in averaged evoked potentials: Monte Carlo comparison of the sensitivity of different methods. *Electroencephalography and Clinical Neurophysiology*, *96*, 574–584.
- Alho, K., Woods, D. L., Algazi, A., & Näätänen, R. (1992). Intermodal selective attention. II. Effects of attentional load on processing of auditory and visual stimuli in central space. *Electroencephalography and Clinical Neurophysiology*, *82*, 356–368.
- American Encephalographic Society. (1994). Guideline thirteen: Guidelines for standard electrode position nomenclature. *Journal of Clinical Neurophysiology*, *11*, 111–113.
- Basar-Eroglu, C., Strüber, D., Stadler, M., & Kruse, E. (1993). Multistable visual perception induces a slow positive EEG wave. *International Journal of Neuroscience*, *73*, 139–151.
- Birbaumer, N., Elbert, T., Canavan, A. G. M., & Rockstroh, B. (1990). Slow potentials of the cerebral cortex and behavior. *Physiological Reviews*, *70*, 1–41.
- Blake, R., & Logothetis, N. K. (2002). Visual competition. *Nature Reviews Neuroscience*, *3*, 13–21.
- Boehm, S. G., Sommer, W., & Lueschow, A. (2005). Correlates of implicit memory for words and faces in event-related brain potentials. *International Journal of Psychophysiology*, *55*, 95–112.
- Brodeur, M., Lepore, F., Veilleux, C., Alyanak, Y., & Debruille, J. B. (2006). Effect of connectivity and bistability on the visual potentials evoked by illusory figures. *NeuroReport*, *17*, 157–161.
- Crick, F., & Koch, C. (1998). Consciousness and neuroscience. *Cerebral Cortex*, *8*, 97–107.
- Di Lollo, V., Enns, J. T., & Rensink, R. A. (2000). Competition for consciousness among visual events: the psychophysics of reentrant visual processes. *Journal of Experimental Psychology: General*, *129*, 481–507.
- Edgington, E. S. (1995). *Randomization tests* (3rd ed). New York: Dekker.
- Engel, A. K., Fries, P., & Singer, W. (2001). Dynamic predictions: Oscillations and synchrony in top-down processing. *Nature Reviews Neuroscience*, *2*, 704–716.
- Fu, S., Fan, S., & Chen, L. (2003). Event-related potentials reveal involuntary processing of orientation changes in the visual modality. *Psychophysiology*, *40*, 770–775.
- Geisser, S., & Greenhouse, S. W. (1958). An extension of Box's results on the use of the *F*-distribution in multivariate analysis. *Annals of Mathematical Statistics*, *29*, 885–891.
- Grossmann, J. K., & Dobbins, A. C. (2006). Competition in bistable vision is attribute-specific. *Vision Research*, *46*, 285–292.
- Holm, S. (1979). A simple sequentially rejective multiple test procedure. *Scandinavian Journal of Statistics*, *6*, 65–70.
- Inui, T., Tanaka, S., Okada, T., Nishizawa, S., Katayama, M., & Konishi, J. (2000). Neural substrates for depth perception of the Necker cube; a functional magnetic resonance imaging study in human subjects. *Neuroscience Letters*, *282*, 145–148.
- James, W. (1950). *Principles of psychology I*. New York: Dover.
- Kleinschmidt, A., Buchel, C., Zeki, S., & Frackowiak, R. S. (1998). Human brain activity during spontaneously reversing perception of ambiguous figures. *Proceedings of the Royal Society of Edinburgh. Section B: Biology*, *265*, 2427–2433.
- Kornhuber, H. H., & Deecke, L. (1965). Hirnpotentialänderungen bei Willkürbewegungen und passiven Bewegungen des Menschen: Bereitschaftspotential und reafferente Potentiale. *Pflügers Archiv für die gesamte Physiologie des Menschen und der Tiere*, *284*, 1–17.
- Kornmeier, J., & Bach, M. (2004). Early neural activity in Necker-cube reversal: Evidence for low-level processing of a gestalt phenomenon. *Psychophysiology*, *41*, 1–8.
- Kornmeier, J., & Bach, M. (2005). The Necker cube—An ambiguous figure disambiguated in early visual processing. *Vision Research*, *45*, 955–960.
- Kornmeier, J., & Bach, M. (2006). Bistable perception—Along the processing chain from ambiguous visual input to a stable percept. *International Journal of Psychophysiology*, *62*, 345–349.
- Kornmeier, J., Heinrich, S. P., Atmanspacher, H., & Bach, M. (2001). The reversing “Necker Wall”—A new paradigm with reversal entrainment reveals an early EEG correlate. Paper presented at the ARVO 2001 Annual Meeting, Fort Lauderdale, Florida, USA.
- Kornmeier, J., Heinrich, S. P., & Bach, M. (2002). Necker-Würfel: Neuronale Sättigung und “top-down” Einflüsse. Paper presented at the 5th Tübinger Wahrnehmungskonferenz, Tübingen, Germany.
- Leopold, D. A., Wilke, M., Maier, A., & Logothetis, N. K. (2002). Stable perception of visually ambiguous patterns. *Nature Neuroscience*, *5*, 605–609.
- Long, G. M., & Toppino, T. C. (2004). Enduring interest in perceptual ambiguity: Alternating views of reversible figures. *Psychological Bulletin*, *130*, 748–768.
- Maier, A., Wilke, M., Logothetis, N. K., & Leopold, D. A. (2003). Perception of temporally interleaved ambiguous patterns. *Current Biology*, *13*, 1076–1085.
- Müller, T. J., Federspiel, A., Horn, H., Lovblad, K., Lehmann, C., Dierks, T., et al. (2005). The neurophysiological time pattern of illusory visual perceptual transitions: A simultaneous EEG and fMRI study. *International Journal of Psychophysiology*, *55*, 299–312.
- Näätänen, R. (1990). The role of attention in auditory information processing as revealed by event-related brain potentials. *Behavioral and Brain Sciences*, *13*, 199–290.
- Necker, L. A. (1832). Observations on some remarkable optical phenomena seen in Switzerland; and on an optical phenomenon which occurs on viewing a figure of a crystal or geometrical solid. *London and Edinburgh Philosophical Magazine and Journal of Science*, *1*, 329–337.
- O'Donnell, B. F., Hendler, T., & Squires, N. K. (1988). Visual evoked potentials to illusory reversals of the Necker cube. *Psychophysiology*, *25*, 137–143.

- Orbach, J., Ehrlich, D., & Heath, H. (1963). Reversibility of the Necker cube: I. An examination of the concept of "satiation of orientation". *Perceptual and Motor Skills*, 17, 439–458.
- Orbach, J., Zucker, E., & Olson, R. (1966). Reversibility of the Necker cube: VII: Reversal rate as a function of figure-on and figure-off durations. *Perceptual and Motor Skills*, 22, 615–618.
- Pelton, L. H., & Solley, C. M. (1968). Acceleration of reversals of a Necker cube. *American Journal of Psychology*, 81, 585–588.
- Pitts, M. A., Nerger, J. L., & Davis, T. J. R. (2007). Electrophysiological correlates of perceptual reversals for three different types of multistable images. *Journal of Vision*, 7, 1–14.
- Regan, D. (1989). *Human brain electrophysiology. Evoked potentials and evoked magnetic fields in science and medicine*. New York: Elsevier.

- Sommer, W., Heinz, A., Leuthold, H., Matt, J., & Schweinberger, S. R. (1995). Metamemory, distinctiveness, and event-related potentials in recognition memory for faces. *Memory and Cognition*, 23, 1–11.
- Strüber, D., & Herrmann, C. S. (2002). MEG alpha activity decrease reflects destabilization of multistable percepts. *Brain Research. Cognitive Brain Research*, 14, 370–382.
- Toppino, T. C. (2003). Reversible-figure perception: Mechanisms of intentional control. *Perception & psychophysics*, 65, 1285–1295.
- World Medical Association. (2000). Declaration of Helsinki: Ethical principles for medical research involving human subjects. *JAMA*, 284, 3043–3045.

(RECEIVED December 18, 2006; ACCEPTED February 28, 2007)

APPENDIX

Least squares estimates of the profile $P_2(t)$ and the parameter α in Equation (1) were obtained as follows. First, let α be fixed. Taking pairwise differences,

$$\Delta_{i,k}R(t) = R(\delta_i, t) - R(\delta_k, t) = P_2(t) \cdot (e^{-\alpha\delta_i} - e^{-\alpha\delta_k}) + \varepsilon_{i,k}(t),$$

removes $P_1(t)$, so the residuals

$$\varepsilon_{i,k}(t) = \Delta_{i,k}R(t) - P_2(t) \cdot (e^{-\alpha\delta_i} - e^{-\alpha\delta_k})$$

involve only the unknown $P_2(t)$. The latter is estimated by minimizing

$$E_\alpha(t) = \sum_{i,k} (\varepsilon_{i,k}(t))^2 = \sum_{i,k} (\Delta_{i,k}R(t) - P_2(t) \cdot g_{i,k}(\alpha))^2 \quad (\text{A1})$$

where $g_{i,k}(\alpha) = e^{-\alpha\delta_i} - e^{-\alpha\delta_k}$. The solution,

$$P_2(t) = \frac{\sum_{i,k} \Delta_{i,k}R(t) \cdot g_{i,k}(\alpha)}{\sum_{i,k} (g_{i,k}(\alpha))^2}, \quad (\text{A2})$$

still depends on α . Inserting (A2) into (A1) and then minimizing the error sum

$$ES = \sum_t E_\alpha(t)$$

with respect to α yields the estimate for parameter α (which here resulted as 0.013), and hence the final estimate of $P_2(t)$. The minimization over α has no explicit closed-form solution, but is easily accomplished by numerical search.

Explained variance is calculated by the formula

$$EV = \frac{(ES_0 - ES)}{ES_0},$$

where

$$ES_0 = \sum_t \sum_{i,k} (R(\delta_i, t) - R(\delta_k, t))^2$$

(and the estimates of $P_2(t)$ and α are substituted in the expression for ES).